# **ChemComm**



### COMMUNICATION

**View Article Online** 



Cite this: Chem. Commun., 2019, 55 8864

Received 15th April 2019, Accepted 13th June 2019

DOI: 10.1039/c9cc02934f

rsc.li/chemcomm

## Bifunctional electrocatalysis for CO<sub>2</sub> reduction via surface capping-dependent metal-oxide interactions\*

Multi-component materials are a new trend in catalyst development for electrochemical CO2 reduction. Understanding and managing the chemical interactions within a complex catalyst structure may unlock new or improved reactivity, but is scientifically challenging. We report the first example of capping ligand-dependent metaloxide interactions in Au/SnO2 structures for electrocatalytic CO2 reduction. Cetyltrimethylammonium bromide capping on the Au nanoparticles enables bifunctional CO2 reduction where CO is produced at more positive potentials and HCOO<sup>-</sup> at more negative potentials. With citrate capping or no capping, the Au-SnO2 interactions steer the selectivity toward H2 evolution at all potentials. Using electrochemical CO oxidation as a probe reaction, we further confirm that the metal-oxide interactions are strongly influenced by the capping ligand.

Electrochemical carbon dioxide (CO<sub>2</sub>) reduction reactions are promising for valorizing CO<sub>2</sub> waste as an abundant and renewable carbon resource and for mitigating the adverse effects of increased CO<sub>2</sub> emissions on the climate. Among all possible products of CO<sub>2</sub> electroreduction, carbon monoxide (CO) and formate (HCOO<sup>-</sup>) are two valuable and easily accessible candidates. 1-3 Extensive research has been carried out to develop active and selective electrocatalysts for converting CO<sub>2</sub> to CO or HCOO<sup>-.2-5</sup> Recent works have gone beyond single-component catalysts to more complex structures, such as bimetallic nanoparticles, 6-8 coreshell structures, 9,10 molecule/nanocarbon hybrids 11,12 and metal/ oxide interfaces113,14 for higher activity and selectivity.

Metal-oxide interactions, a concept extensively studied for gas-phase catalysis, 15-17 has recently been investigated for enhancing electrocatalysis of CO<sub>2</sub> reduction. 10,13,14,18-20 Both metals and metal oxides can be active catalysts for electrochemical CO2 reduction

reactions. Given the observation that CO can be produced by metal catalysts in the more positive potential region whereas HCOO is formed on oxidized metal surfaces at more negative potentials, 21 it is possible to construct a CO/HCOO<sup>-</sup> bifunctional catalyst consisting of one metal and one metal oxide as active components, whose selectivity can be controlled by the applied potential. We have recently demonstrated such a catalyst utilizing win-win metal-oxide (Ag-SnO<sub>x</sub>) cooperation that boosts both the CO<sub>2</sub>-to-CO catalysis on the metal and the CO<sub>2</sub>-to-HCOO<sup>-</sup> catalysis on the oxide. 13 Despite this progress, bifunctional CO<sub>2</sub> reduction electrocatalysts are still rare, possibly associated with the difficulty in managing multicomponent interactions within a catalyst structure. A deeper understanding of the metal-oxide interactions and their influences on catalytic properties, therefore, entails further investigation.

In this work, we studied different composites of Au and SnO<sub>2</sub> nanoparticles for CO2 electroreduction. The Au-SnO2 interactions were found to be strongly dependent on the capping ligand of the Au nanoparticles. In contact with SnO2 nanoparticles supported on carbon nanotubes (SnO2/CNT), both the capping-free Au (CF-Au) and citrate-capped Au (Cit-Au) nanoparticles give rise to adverse interactions that favor the competing hydrogen evolution reaction (HER). A substantial amount of H<sub>2</sub> is produced in the potential range of -0.50 to -1.00 V vs. RHE. When the cetyltrimethylammonium bromide-capped Au (CTAB-Au) nanoparticles are used instead, HER is suppressed. The catalyst manifests a high selectivity for CO at -0.50 V and for HCOO<sup>-</sup> at -0.90 V, enabling bifunctional CO₂ reduction behavior. Using electrooxidation of CO as a probe reaction, we further show that the Au sites on the surface of CTAB-Au/SnO2 are different from those of CF-Au/SnO<sub>2</sub> or Cit-Au/SnO<sub>2</sub>. To the best of our knowledge, this is the first report on tailoring metal-oxide interactions and electrocatalytic properties via changing the capping ligand at the metal/oxide interface.

The Au/SnO<sub>2</sub> system without the capping ligand was first investigated. Prior to the construction and measurement of this binary system, CF-Au and SnO2 nanoparticles were respectively grown on CNTs (Fig. S1 and S2, ESI†) for their intrinsic catalytic properties for CO2 electroreduction to be assessed. CNTs are a

<sup>&</sup>lt;sup>a</sup> Department of Chemistry, Yale University, New Haven, Connecticut 06520, USA. E-mail: hailiang.wang@yale.edu

<sup>&</sup>lt;sup>b</sup> Energy Sciences Institute, Yale University, West Haven, Connecticut 06516, USA

<sup>&</sup>lt;sup>c</sup> Institute of Functional Nano and Soft Materials (FUNSOM), Jiangsu Key Laboratory for Carbon-Based Functional Materials and Devices, Soochow University, Suzhou, China

<sup>†</sup> Electronic supplementary information (ESI) available. See DOI: 10.1039/c9cc02934f

Communication ChemComm

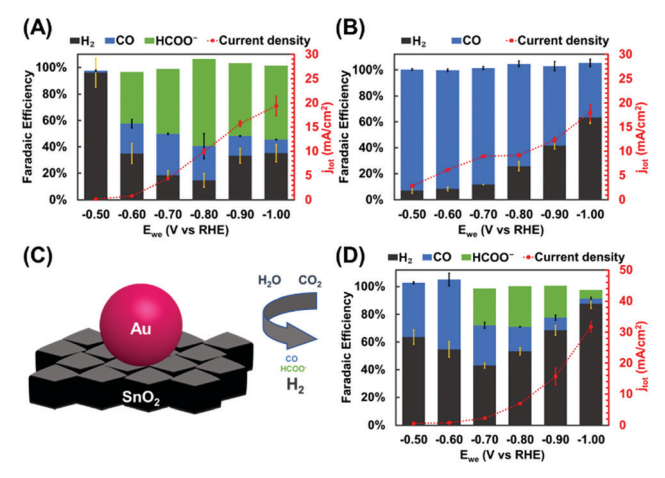


Fig. 1 Potential-dependent catalytic performance of (A) SnO<sub>2</sub> and (B) CF-Au for the electroreduction of CO<sub>2</sub>. (C) Schematic illustration and (D) potentialdependent catalytic performance of CF-Au/SnO2 for the electroreduction of CO<sub>2</sub>. Error bars represent standard deviations from multiple measurements.

widely used support in electrocatalysis due to their high electrical conductivity and large surface area. 18,22 In 0.5 M aqueous KHCO<sub>3</sub>, SnO<sub>2</sub> catalyzes CO<sub>2</sub> reduction to HCOO<sup>-</sup> with an onset potential of -0.60 V vs. RHE. The highest faradaic efficiency (FE) for  $HCOO^{-}$  is 66% achieved at -0.80 V with a total current density  $(j_{\text{total}})$  of 9.91 mA cm<sup>-2</sup> (Fig. 1A). CF-Au catalyzes CO<sub>2</sub> reduction to CO with the highest FE<sub>CO</sub> of 93% and a  $j_{\text{total}}$  of 2.80 mA cm<sup>-2</sup> at -0.50 V (Fig. 1B). These activity and selectivity results agree well with reports on Au and SnO<sub>2</sub> in the literature. <sup>23,24</sup> The CF-Au/ SnO<sub>2</sub> catalyst was constructed by growing CF-Au nanoparticles onto SnO<sub>2</sub>/CNT (Fig. 1C and Fig. S3, ESI†). To our surprise, the catalytic performance of CF-Au/SnO2 toward CO2 reduction is far worse than a simple combination of CF-Au and SnO<sub>2</sub>. H<sub>2</sub> is the major product throughout the potential range examined (Fig. 1D). The highest  $FE_{HCOO^-}$  and  $FE_{CO}$  are only 29% and 50%,

We then explored the possibility of utilizing surface capping to modify metal-oxide interactions and to influence electrocatalytic CO<sub>2</sub> reduction. CTAB-Au nanoparticles were synthesized (Fig. S2 and S4A, ESI†). They exhibit similar catalytic activity and selectivity toward CO<sub>2</sub>-to-CO conversion as the CF-Au nanoparticles (Fig. S5A, ESI†). Remarkably, the CTAB-Au/SnO<sub>2</sub> mixture (Fig. 2A and Fig. S6A, B, ESI†) exhibits a potential-dependent bifunctional behavior for CO<sub>2</sub> electroreduction (Fig. 2B). In the lower overpotential range, CO is the dominant product. At -0.50 V vs. RHE, CO is produced with  $FE_{CO} = 96\%$  and a  $j_{CO}$  of 0.26 mA cm<sup>-2</sup>. In the more negative potential range, HCOO<sup>-</sup> is the major product, with the highest  $FE_{HCOO^-} = 65\%$  achieved at -0.90 V together with a  $j_{HCOO^-}$  of  $6.66 \text{ mA cm}^{-2}$ . HER is suppressed to <15% in FE in the potential range between -0.50 V and -0.90 V. As a comparison, we prepared Cit-Au nanoparticles from the CTAB-Au nanoparticles via a reported ligand exchange method.<sup>25</sup> The absence of N element on the surface of the obtained Cit-Au nanoparticles, as revealed by X-ray photoelectron spectroscopy (XPS), verifies successful substitution of CTAB with citrate ions (Fig. S7, ESI†). While Cit-Au shows similar electrocatalytic

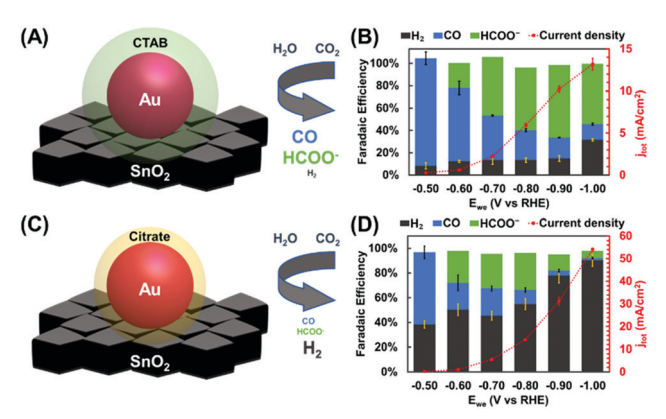


Fig. 2 (A and C) Schematic illustration and (B and D) potential-dependent catalytic performance of (A and B) CTAB-Au/SnO2 and (C and D) Cit-Au/ SnO<sub>2</sub> for the electroreduction of CO<sub>2</sub>. Error bars represent standard deviations from multiple measurements

properties as CTAB-Au (Fig. S5B, ESI†), the Cit-Au/SnO<sub>2</sub> mixture (Fig. 2C and Fig. S6C, D, ESI†) exhibits a poor selectivity for both CO and HCOO<sup>-</sup> (Fig. 2D). At -0.50 V, FE<sub>CO</sub> is only 58%. At -0.90 V, FE<sub>H<sub>2</sub></sub> reaches 78% and FE<sub>HCOO</sub> is below 15%. This behavior is very similar to the case of the CF-Au/SnO2 catalyst (Fig. 1D), where HER dominates the reduction current in the entire potential range examined.

To understand the different catalytic properties of the three Au/SnO2 systems, we performed a linear combination analysis to quantitatively capture the change of HER activity caused by the metal-oxide interactions as a function of the capping ligand on Au. We assume that in each Au/SnO2 system the Au and SnO<sub>2</sub> components work independently and that the catalytic performance of the mixture is a simple addition of the two. Based on the fact that Au is predominant for CO production in the lower overpotential range and that SnO2 provides the sole active sites for HCOO- production, the active contents of Au and SnO2 in each Au/SnO2 system are determined from the experimentally measured CO and HCOO- production rates at -0.50 V and -0.80 V, respectively (Table S1, ESI†). Then the linear combination HER rate is calculated. Fig. 3 compares FE<sub>H<sub>2</sub></sub> and  $j_{\rm H_2}$  calculated from the linear combination analysis with the experimentally measured values for CF-Au/SnO<sub>2</sub>, CTAB-Au/SnO<sub>2</sub> and Cit-Au/SnO2. For all three catalysts, the actual values deviate significantly from the linear combination values, suggesting that the Au-SnO<sub>2</sub> interactions strongly affect the catalysis. Notably, the three fall into two categories. For CTAB-Au/SnO2, not only is the selectivity toward H<sub>2</sub> suppressed but also the reaction rate is notably lower than the simple addition of CTAB-Au and SnO2 (Fig. 3C and D). In contrast, CF-Au/SnO<sub>2</sub> and Cit-Au/SnO<sub>2</sub> both exhibit significantly higher activity and selectivity for the HER (Fig. 3A, B, E and F). These results support our conclusion that the surface capping ligands of the Au nanoparticles strongly influence the interactions with SnO2 and consequently alter the electrocatalytic properties for CO2 reduction. In particular, CTAB mediates desirable Au-SnO2 interactions and enables productselectable dual-mode CO2 electroreduction to CO and HCOOover a single catalyst.

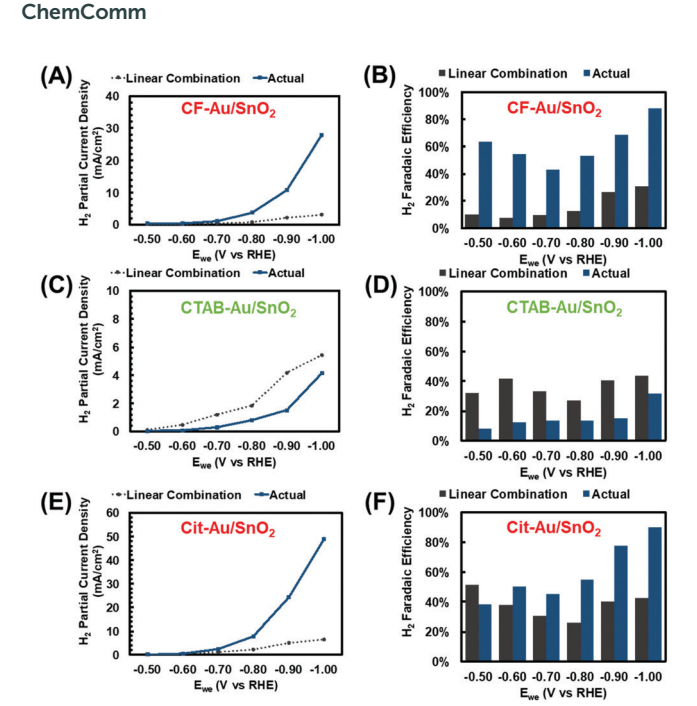


Fig. 3 Comparison of (A, C and E)  $j_{\rm H_2}$  and (B, D and F) FE<sub>H2</sub> between actual values and values calculated from the linear combination analysis for (A and B) CF-Au/SnO<sub>2</sub>, (C and D) CTAB-Au/SnO<sub>2</sub> and (E and F) Cit-Au/SnO<sub>2</sub>.

It is interesting to note that CF-Au, CTAB-Au and Cit-Au possess very similar catalytic properties for CO<sub>2</sub> electroreduction (Fig. 1B and Fig. S5, ESI†), yet their interactions with SnO<sub>2</sub> are quite different. While surface capping-dependent electrocatalytic activity and selectivity has been reported for Pt nanoparticles toward the oxygen reduction reaction, <sup>26</sup> this is the first time that capping ligand-mediated metal–oxide interactions in electrocatalysis are discovered. To further study how the metal–oxide interactions alter the properties of the catalytic sites, we chose electrooxidation of CO as a probe reaction to characterize the surface Au sites of the three Au/SnO<sub>2</sub> catalysts. <sup>27–29</sup> The Au nanoparticles are known to catalyze CO electrooxidation in

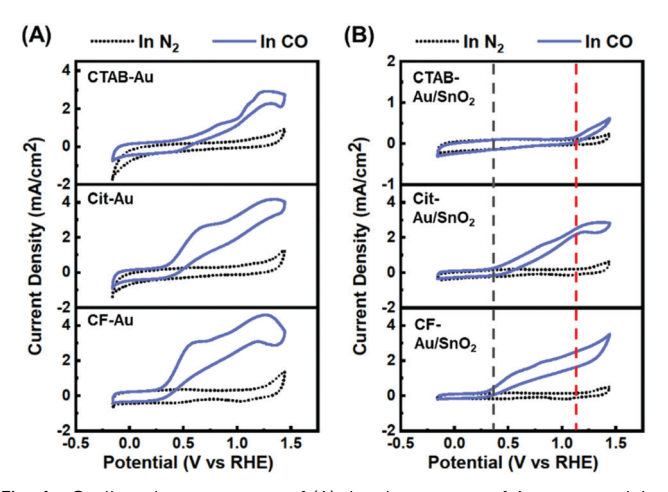


Fig. 4 Cyclic voltammograms of (A) the three types of Au nanoparticles with different surface capping states and (B) the three Au/SnO $_2$  catalysts in N $_2$  and in CO in 0.5 M aqueous KHCO $_3$ . Scan rate: 50 mV s $^{-1}$ .

neutral aqueous solutions. Cyclic voltammograms were first recorded in CO-saturated 0.5 M aqueous KHCO3 for the three kinds of Au nanoparticles with different capping states and the SnO<sub>2</sub> nanoparticles. SnO<sub>2</sub> itself is inactive toward CO electrooxidation of CO (Fig. S8, ESI†). The three kinds of Au nanoparticles exhibit almost identical onsets of CO oxidation at  $\sim 0.40$  V vs. RHE (Fig. 4A), in line with earlier reports on CO electrooxidation on the Au surface. 29,30 This indicates that these Au nanoparticles with different capping states possess surface sites with similar chemical properties, which agrees with the observation that they show almost identical catalytic properties for CO<sub>2</sub> reduction. Coupled with SnO<sub>2</sub>, the electrocatalytic activity of both CF-Au and Cit-Au for CO oxidation remains largely unaffected. The CTAB-Au/SnO2, however, shows a much more positive onset potential at  $\sim 1.10$  V. The drastically different activity of CTAB-Au/SnO2 for CO electrooxidation confirms that the metal-oxide interactions in this catalyst are indeed different from those in the other two Au/SnO2 systems, which is consistent with the CO<sub>2</sub> electroreduction results. Given that the proposed ratedetermining step for CO oxidation on Au involves the process of one-electron oxidation of the surface-adsorbed CO,31,32 a more positive onset of this reaction implies increased CO binding affinity, which could be responsible for the observed HER suppression.

In summary, we for the first time demonstrated capping ligand-dependent metal–oxide interactions in electrocatalysis. The catalytic properties of our  $\rm Au/SnO_2$  model systems toward the electrochemical  $\rm CO_2$  reduction reactions are strongly influenced by the presence and identity of the capping ligands on the Au nanoparticles. Without the capping ligands or with citrate as the capping ligand, HER is favored. With CTAB as the capping ligand, HER is suppressed and potential-dependent bifunctional catalysis toward CO and  $\rm HCOO^-$  is realized.

This work was supported by the U.S. National Science Foundation (Grant CHE-1651717).

#### Conflicts of interest

There are no conflicts to declare.

### Notes and references

- 1 J. M. Spurgeon and B. Kumar, Energy Environ. Sci., 2018, 11, 1536-1551.
- 2 J. Qiao, Y. Liu, F. Hong and J. Zhang, Chem. Soc. Rev., 2014, 43, 631-675.
- 3 J. Artz, T. E. Müller, K. Thenert, J. Kleinekorte, R. Meys, A. Sternberg, A. Bardow and W. Leitner, *Chem. Rev.*, 2018, **118**, 434–504.
- 4 R. Francke, B. Schille and M. Roemelt, Chem. Rev., 2018, 118, 4631-4701.
- 5 W. Zhang, Y. Hu, L. Ma, G. Zhu, Y. Wang, X. Xue, R. Chen, S. Yang and Z. Jin, Adv. Sci., 2018, 5, 1700275.
- 6 D. Kim, J. Resasco, Y. Yu, A. M. Asiri and P. Yang, Nat. Commun., 2014, 5, 4948.
- 7 R. Kortlever, I. Peters, S. Koper and M. T. M. Koper, *ACS Catal.*, 2015, 5, 3916–3923.
- 8 Z. Chang, S. Huo, W. Zhang, J. Fang and H. Wang, J. Phys. Chem. C, 2017, 121, 11368–11379.
- 9 K. Sun, T. Cheng, L. Wu, Y. Hu, J. Zhou, A. Maclennan, Z. Jiang, Y. Gao, W. A. Goddard and Z. Wang, J. Am. Chem. Soc., 2017, 139, 15608–15611.
- 10 W. Luc, C. Collins, S. Wang, H. Xin, K. He, Y. Kang and F. Jiao, J. Am. Chem. Soc., 2017, 139, 1885–1893.
- 11 X. Zhang, Z. Wu, X. Zhang, L. Li, Y. Li, H. Xu, X. Li, X. Yu, Z. Zhang and Y. Liang, *Nat. Commun.*, 2017, **8**, 14675.

- Communication ChemComm
- 12 M. Wang, L. Chen, T.-C. Lau and M. Robert, *Angew. Chem., Int. Ed.*, 2018, 57, 7769–7773.
- 13 Z. Cai, Y. Wu, Z. Wu, L. Yin, Z. Weng, Y. Zhong, W. Xu, X. Sun and H. Wang, ACS Energy Lett., 2018, 3, 2816–2822.
- 14 Q. Li, J. Fu, W. Zhu, Z. Chen, B. Shen, L. Wu, Z. Xi, T. Wang, G. Lu, J.-j. Zhu and S. Sun, J. Am. Chem. Soc., 2017, 139, 4290–4293.
- 15 M. Behrens, F. Studt, I. Kasatkin, S. Kühl, M. Hävecker, F. Abild-Pedersen, S. Zander, F. Girgsdies, P. Kurr, B.-L. Kniep, M. Tovar, R. W. Fischer, J. K. Nørskov and R. Schlögl, Science, 2012, 336, 893–897.
- 16 J. A. Rodriguez, S. Ma, P. Liu, J. Hrbek, J. Evans and M. Pérez, Science, 2007, 318, 1757–1760.
- 17 K. An, S. Alayoglu, N. Musselwhite, S. Plamthottam, G. Melaet, A. E. Lindeman and G. A. Somorjai, J. Am. Chem. Soc., 2013, 135, 16689–16696.
- 18 S. Huo, Z. Weng, Z. Wu, Y. Zhong, Y. Wu, J. Fang and H. Wang, ACS Appl. Mater. Interfaces, 2017, 9, 28519–28526.
- 19 G. O. Larrazábal, A. J. Martín, S. Mitchell, R. Hauert and J. Pérez-Ramírez, ACS Catal., 2016, 6, 6265–6274.
- 20 S. Chu, P. Ou, P. Ghamari, S. Vanka, B. Zhou, I. Shih, J. Song and Z. Mi, J. Am. Chem. Soc., 2018, 140, 7869–7877.
- 21 G. O. Larrazábal, A. J. Martín and J. Pérez-Ramírez, J. Phys. Chem. Lett., 2017, 8, 3933–3944.

- 22 Z. Weng, W. Liu, L.-C. Yin, R. Fang, M. Li, E. I. Altman, Q. Fan, F. Li, H.-M. Cheng and H. Wang, *Nano Lett.*, 2015, 15, 7704–7710.
- 23 S. Zhang, P. Kang and T. J. Meyer, J. Am. Chem. Soc., 2014, 136, 1734–1737.
- 24 H. Mistry, R. Reske, Z. Zeng, Z.-J. Zhao, J. Greeley, P. Strasser and B. R. Cuenya, J. Am. Chem. Soc., 2014, 136, 16473–16476.
- 25 J. G. Mehtala, D. Y. Zemlyanov, J. P. Max, N. Kadasala, S. Zhao and A. Wei, *Langmuir*, 2014, 30, 13727–13730.
- 26 W. Liu and H. Wang, Surf. Sci., 2016, 648, 120-125.
- 27 B. E. Hayden, D. Pletcher, M. E. Rendall and J.-P. Suchsland, J. Phys. Chem. C, 2007, 111, 17044–17051.
- 28 P. Rodriguez, D. Plana, D. J. Fermin and M. T. M. Koper, J. Catal., 2014, 311, 182–189.
- 29 B. B. Blizanac, M. Arenz, P. N. Ross and N. M. Marković, J. Am. Chem. Soc., 2004, 126, 10130–10141.
- 30 H. Kita, H. Nakajima and K. Hayashi, J. Electroanal. Chem. Interfacial Electrochem., 1985, 190, 141–156.
- 31 S. C. Chang, A. Hamelin and M. J. Weaver, J. Phys. Chem., 1991, 95, 5560–5567.
- 32 G. J. Edens, A. Hamelin and M. J. Weaver, J. Phys. Chem., 1996, 100, 2322–2329.